Electronic Supplementary Material (ESI) for CrystEngComm.

Supporting Information for:

Insights into the initial stages of lipid-mediated haemozoin nucleation

David Kuter, Roxanne Mohunlal, Sharné-Maré Fitzroy, Constance Asher, Peter J. Smith, Timothy J. Egan* and Katherine A. de Villiers*

Contents

1. TLC analysis of Hz crystals

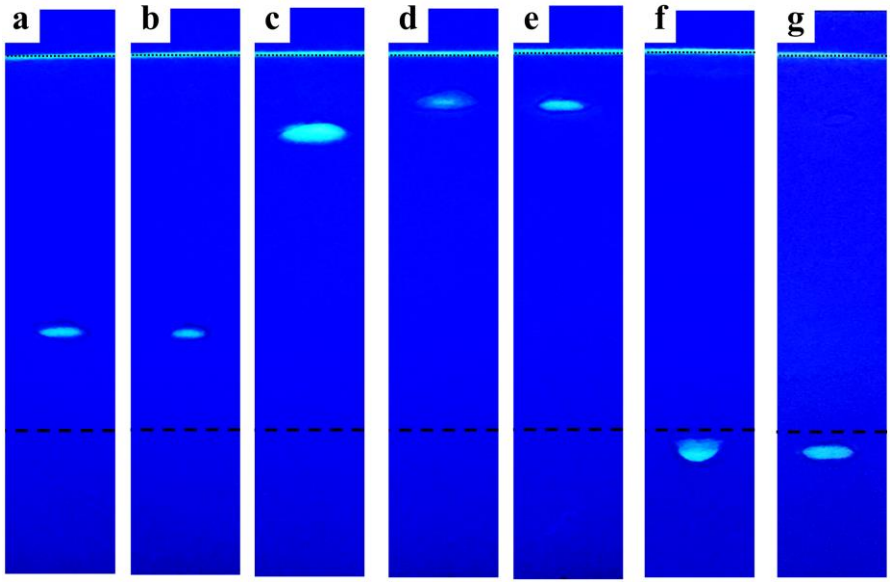

Fig. S1 TLC silica gel plates of neutral glycerolipid standards stained using Primuline. (a) Monostearate glycerol, MSG; (b) monopalmitin glycerol, MPG; (c) dipalmitin glycerol, DPG; (d) dioleoyl glycerol DOG; (e) dilinoleoyl glycerol, DLG; (f) dioleoyl phosphatidylcholine, DOPC; (g) dimyristoyl phosphatidylethanolamine, DMPE. Dashed and dotted lines represent the first and second solvent front respectively.

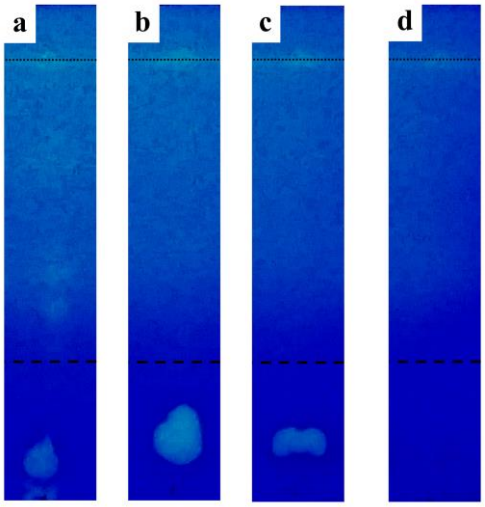

Fig. S2 Lipids extracted from the second (a) and fifth (b) washings of Hz crystals with a 4% (w/v) SDS solution and first (c) and fifth (d) washings of Hz crystals with PBS.

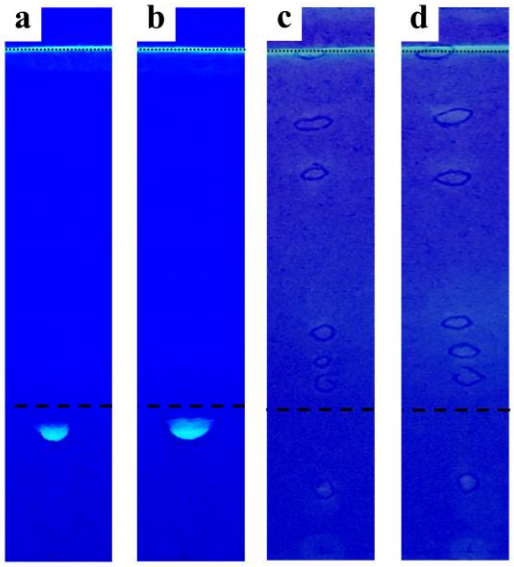

Fig. S3 DOPC (a and b) and parasite lysate (c and d) in the presence (a and c) and absence (b and d) of 0.1 M NaOH.

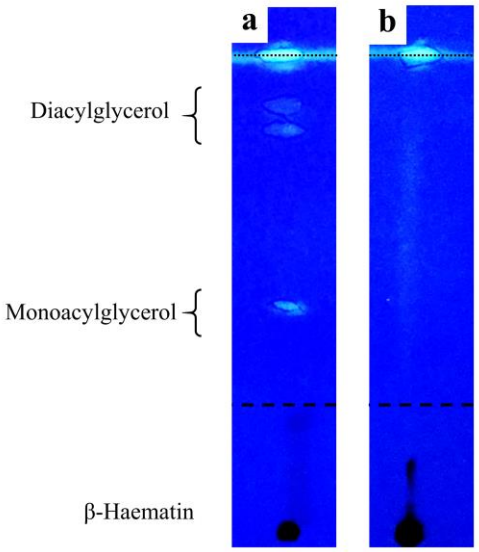

Fig. S4 TLC silica gel plates of β-haematin crystals incubated in the glycerolipid mixture reported by Pisciotta et al.[1] and stained using Primuline. (a) Crystals dissolved without washing; (b) crystals dissolved after extensive washing.

2. Electron microscopy and powder X-ray diffraction analysis

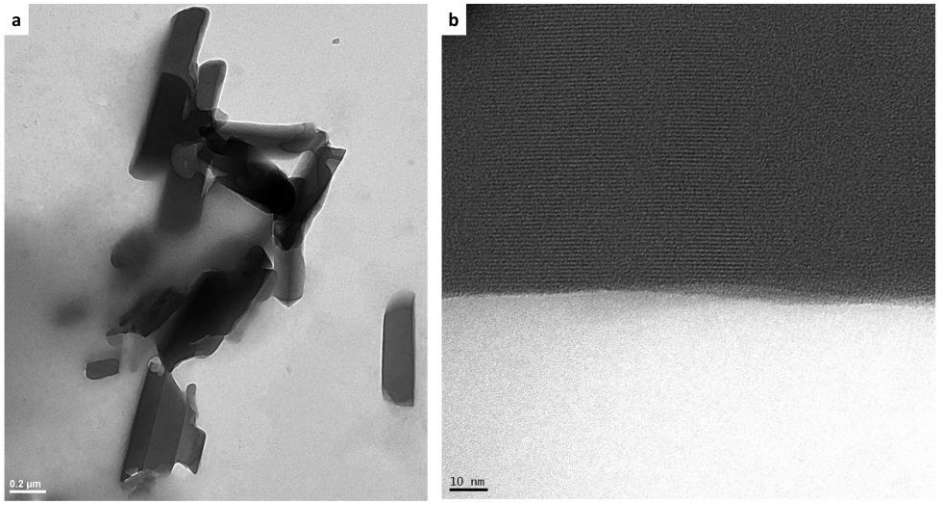

Fig. S5 Transmission electron micrographs of Hz isolated from *P. falciparum* that has been washed with 4% SDS solution. Crystals are lath-shaped (a) and have very regular lattice fringes (b).

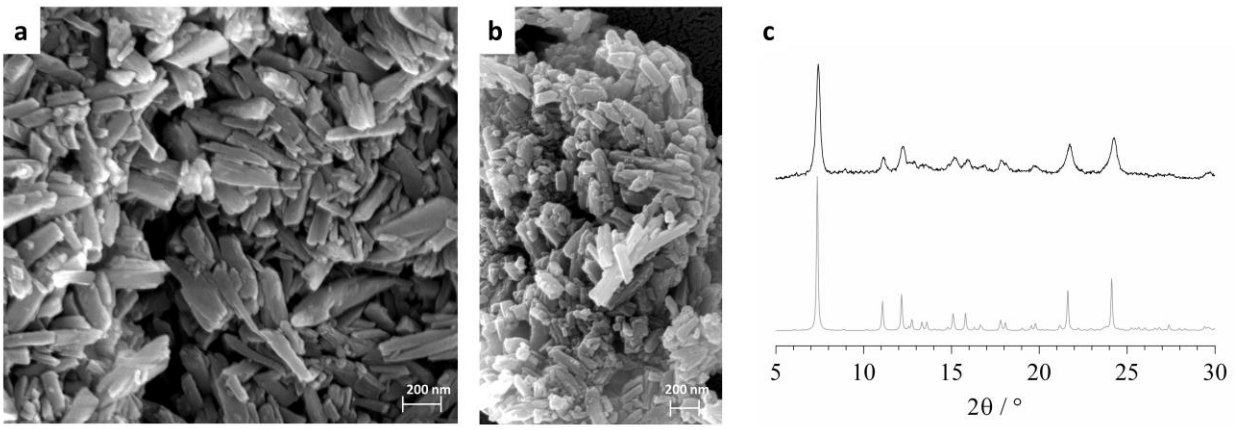

Fig. S6 Scanning electron micrographs (a and b) and powder X-ray diffraction pattern (c) of β-haematin prepared from acetate solution show that the sample is crystalline. In (c), the powder pattern calculated from the reported crystal structure[2] is shown in grey.

3. β-Haematin formation

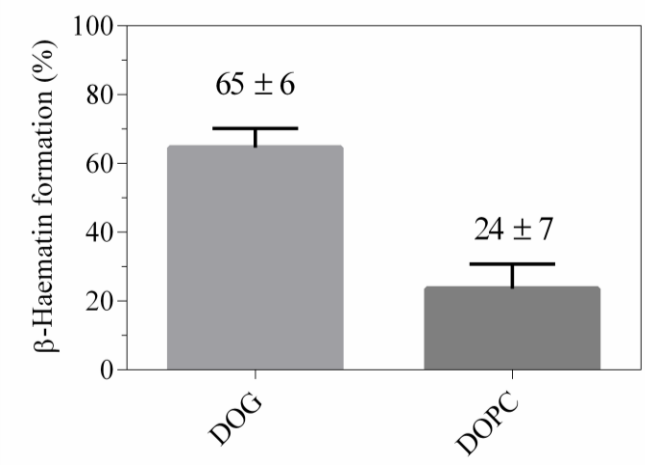

Fig. S7 β-Haematin production mediated by the glycerolipid 1,2-dioleoyl-*sn*-glycerol (DOG) or the phospholipid 1,2-dioleoyl-*sn*-glycero-3-phosphatidylcholine (DOPC) after a 4-hour incubation period at 37 °C.

4. Force field parameterisation

μ-Propionato ferrihaem dimer. A new CHARMM residue was created to describe the μ-propionato ferrihaem dimer (HMZN). Parameterisation of this ferrihaem species was approached in the same manner as previously reported for the μ-oxo ferrihaem dimer[3] where atomic charges were adjusted using the FitCharge module in CHARMM so as to produce a molecular mechanical (MM) electrostatic surface potential (ESP) in good agreement with its quantum mechanical (QM) counterpart (Fig. S8).

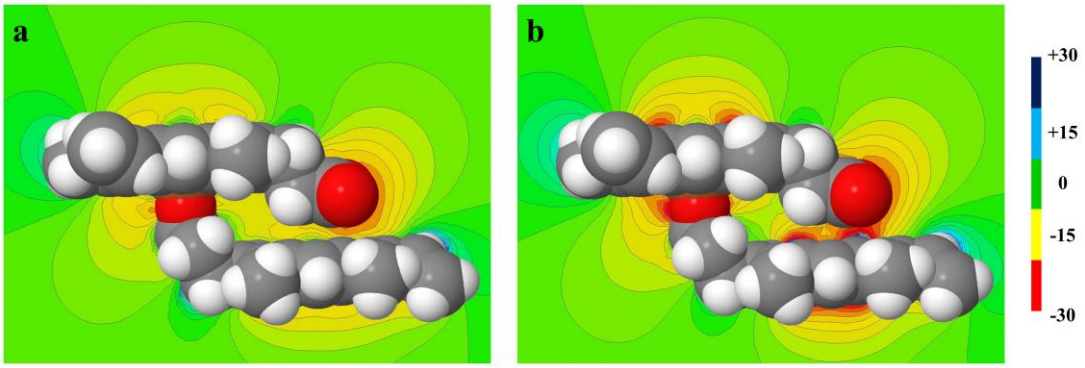

Fig. S8 Electrostatic surface potentials produced from (a) QM (OPBE/LAN2DZ) calculation and (b) MM-optimized atomic charges. Energy is given in kcal mol^{-1} on the right.

Water interaction energies could not be used in atomic charge parameterisation owing to spin contamination obtained in QM calculations (OPBE/LANL2DZ). It should be noted that the optimised QM structure was noticeably different to that reported for β-haematin[2,4] despite the latter being used as the input geometry. In the two reported crystal structures of β-haematin, propionic acid side chains either hydrogen bond to a DMSO solvent molecule[4] or neighbouring ferriheme dimer.[2] On the other hand, the QM structure displayed hydrogen bonding between the propionic acid side chains and the carbonyl oxygen atom of the coordinated propionate group, similar to that observed in the reported crystal structure of the μ-propionato dimer of gallium(III) protoporphyrin IX.[5] This QM geometry obtained was unsurprising given calculations were conducted on a single molecule which lacked hydrogen bonding competitors such as solvent and neighbouring molecules. Final optimized atomic charges are listed in Table S1 and are labelled according to Fig. S9.

Table S1 Optimized atomic charges of the μ-propionato ferrihaem dimer [a, b]

Atom	Atomic charge	
Fe	1.071	
N	-0.576	
C_{α}	0.255	
C_{β}	0.021	
C_{meso}	-0.214	
H_{meso}	0.133	
C_{methyl}	-0.327	
$C_{vinyl-1}$	-0.123	
$H_{vinyl-1}$	0.107	
$C_{vinyl-2}$	-0.274	
$H_{vinyl-2}$	0.123	
	Coordinated propionate	*Unligated propionic acid*
C_{prop-1}	-0.232	-0.212
C_{prop-2}	-0.222	-0.226
CO	0.470	0.437
C=O	-0.359	-0.270
O_{lig}/OH	-0.421	-0.377
H	-	0.357

[a] See Fig. S9 for atom labelling; [b] aliphatic H atoms have charges of 0.090 e.

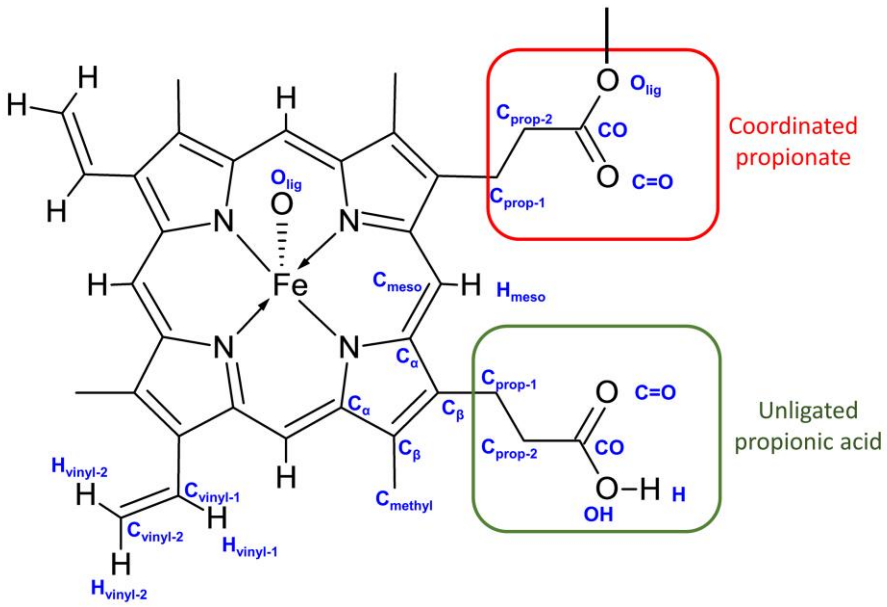

Fig. S9 Atom labelling for one porphyrin of the μ-propionato ferrihaem dimer. Non-polar hydrogens omitted for clarity.

The Fe-coordinated propionate oxygen atom of μ-propionato ferrihaem was described by the same atom type used for HO-ferrihaem.[3] All parameters initially used were the same as those employed for HO-ferrihaem except for the Fe-O-C angle which required new structural parameters. With the exception of the Fe-O bond length and N-Fe-O angle, parameters produced an MM geometry in good agreement with the structure obtained from QM calculation. Force constants and reference bond/angle parameters describing the Fe-O bond length and N-Fe-O angle were modified (Table S2) such that these descriptors were in agreement with target values in both HO-ferrihaem and μ-propionato ferriheme. The mean unsigned error (MUE) in bond lengths and angles between CHARMM and target values was 0.02 Å and 1° respectively, and with the exception of the Fe-O bond length, the MUE did not exceed 0.03 Å or 3°. While the optimized Fe-O bond length (1.88 Å) is somewhat shorter than the target QM value (1.92 Å), it is in good agreement with experimental

values (1.89 and 1.90 Å). Selected bond lengths and angles for the μ-propionato ferriheme dimer are given in Table S3. In the case of the N-Fe-O angle, the force constant used was the same as that previously employed for μ-oxo ferriheme. Given its ability to correctly describe this angle in HO-ferrihaem, μ-oxo ferrihaem and μ-propionato ferrihaem, the corresponding angle in H_2O-ferrihaem was re-parameterised using this value and a modified reference angle (Table S2).

Table S2 Modified ferrihaem parameters

	Force Constant	**Reference bond/angle**
Fe-O [a]	350.0 kcal mol^{-1} $Å^{-2}$	1.92 Å
Fe-O-C [b]	55.0 kcal mol^{-1} rad^{-2}	165.0 °
N-Fe-O [a]	139.3 kcal mol^{-1} rad^{-2}	103.0 °
N-Fe-O [c]	139.3 kcal mol^{-1} rad^{-2}	100.0 °

[a] For μ-propionato and HO-ferrihaem; [b] For μ-propionato ferrihaem only; [c] For H_2O-ferrihaem.

Table S3 Selected average bond lengths and angles of μ-propionato ferrihaem obtained using optimized CHARMM parameters compared to corresponding values in the QM structure [a]

	QM (OPBE/LANL2DZ)	**CHARMM**
Fe-O	1.922 Å	1.879 Å
Fe-N	2.094(5) Å	2.103(2) Å
Fe-O-C	167.3(8) °	163.91(3) °
N-Fe-O	102(2) °	103.9(4) °
N-Fe-N	87.4(2)/155.2(3) °	86.7(6)/152.2(1) °
Fe-N-C_α	126.3(4) °	126.7(4) °

[a] Standard deviation given in parenthesis where possible

DOG. A new CHARMM residue was created to describe dioleoylglycerol. The topology DOPC in the original CHARMM force field was used as a template but the phosphocholine headgroup was replaced by a single hydrogen atom attached to O_{11} (see Fig. S10). The hydrogen atom (H_L) and O_{11} atom types were set to those describing the glycerol moiety in the dilauroyl-glycero-phosphoglycerol residue described in the CHARMM lipid force field (DLPG).[6] Atomic charges for H_L, O_{11} and carbon atom directly attached to O_{11} (C_1) were given the same values as the corresponding atoms in DLPG (H_{O3}, O_{C3} and C_{13} respectively). No additional structural parameterization was required. To create a DOG bilayer, coordinates of a DOPC bilayer were edited. Atomic coordinates of N, H_{11A}, O_{13}, H_{13C}, O_{14}, H_{14A} and H_{15A} atoms (see Fig. S10) were removed; atom type P was renamed H_L; atoms C_{11}, C_{12}, C_{13}, C_{14} and C_{15} were renamed to the oxygen atom of solvent water (O_{H2}); and atoms H_{11B}, O_{12}, H_{12A}, H_{12B}, H_{13A}, H_{13B}, H_{14B}, H_{14C}, H_{15B} and H_{15C} were renamed to hydrogen atoms of solvent water molecules (H_1 and H_2). Systems were minimized in CHARMM and NAMD as reported in the main text, followed by 10 ns equilibrium dynamics and 100 ns production dynamics MD simulations using NAMD.

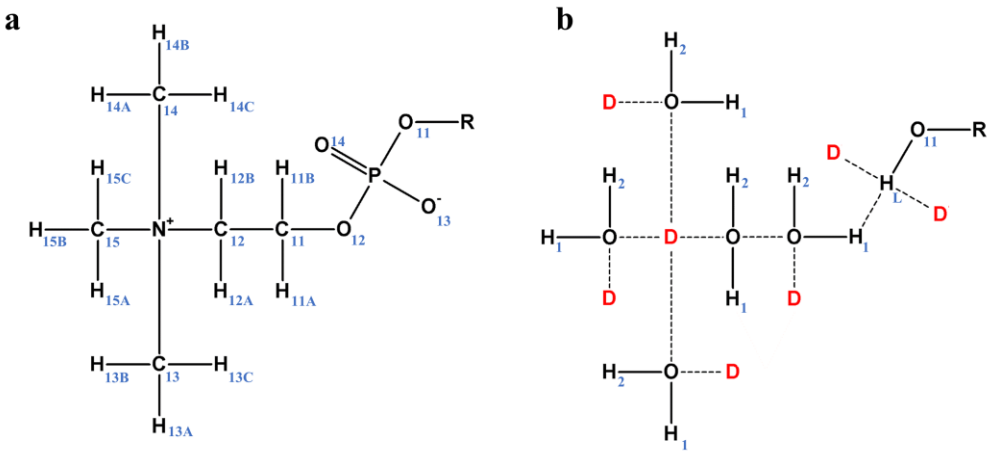

Fig. S10 Atomic coordinates of the phosphatidylcholine headgroup of DOPC (a) edited to produce DOG (b). Numbering and labelling corresponds to CHARMM nomenclature. Positions labelled "D" in (b) indicate deleted atoms.

5. Analysis of MD simulations

5.1 Density profiles

Coordinates of MD trajectories were reduced to a single dimension perpendicular to the lipid surface (defined as the z-axis) after which radial distribution function calculations were conducted in CHARMM. The density profiles of lipid headgroups and ester groups were calculated relative to the centre of the bilayer. In the case of DOPC, non-hydrogen atoms of the phosphatidylcholine headgroup were employed while the oxygen atom of the glycerol headgroup was used for DOG. Density profiles of double bonded carbon atoms in the lipid tail were determined relative the headgroup region and the distance adjusted so as to become referenced to the bilayer centre. Density profiles of ferriheme dimers were calculated using non-hydrogen atoms of the porphyrin core (excluding axial ligands) relative to either the centre of the bilayer in the case of the π-π dimer or headgroups in the case of the μ-propionato dimer and the distance adjusted where necessary. Profiles were only determined using frames in which the ferrihaem dimers had penetrated the lipid bilayers.

5.2 Distance from lipid

To determine the distance of ferrihaem dimers from the lipid (Fig. S11), the least squares plane through the lipid headgroups and centre of mass (COM) of the porphine core of each ferrihaem molecule in the dimer (excluding hydrogen atoms) was determined for each frame in the MD simulation. The distance of the ferrihaem COM to an equivalent point on the plane of the lipid headgroups was calculated using equation 1, where the general equation of the plane is $ax + by + cz + d = 0$ and coordinates of the COM are (x_0, y_0, z_0). Calculated distances of each ferrihaem monomer in the dimer were averaged per frame. To reference values relative to the centre of a bilayer, 17.5

and 19 Å were added to the calculated distances in DOG and DOPC systems respectively. These values were determined from the peak position of density profiles calculated for the lipid headgroups above.

$$r = \frac{|ax_0+by_0+cz_0+d|}{\sqrt[2]{a^2+b^2+c^2}} \quad (1)$$

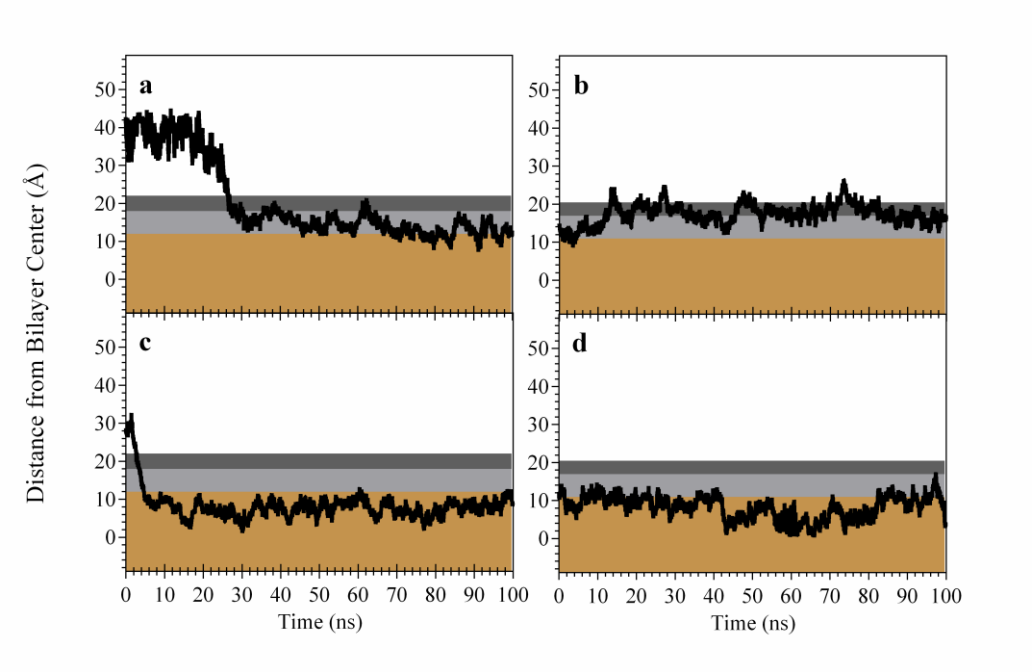

Fig. S11 Distance of ferrihaem π-π dimers (a and b) and μ-propionato dimers (c and d) from the centre of DOPC (left) and DOG bilayers (right) over the course of MD simulation. Data are reported for ferrihaem dimers placed in the bulk aqueous phase at the start of MD simulation. Penetration of ferrihaem dimers into DOG occurred during the equilibration period and are not shown. To aid visualization, phosphatidylcholine and glycerol headgroup regions have been shaded dark grey, ester groups in light grey and tail regions in brown. Bulk aqueous solvent is represented by the white area above the bilayer.

5.3 Hydrogen bonding contacts

Hydrogen bonding contacts were determined for each frame of the between various moieties in the ferrihaem dimer and solvent, lipid headgroup or ester group atoms. Only frames in which the ferrihaem dimer had penetrated the lipid bilayer were used. The formation of a hydrogen bond contact was defined when the O – H or O – N^+ distance was ≤ 2.4 or 3.5 Å respectively. The average contacts over the course of the simulation are reported per ferrihaem dimer.

6. Density functional theory calculations

Table S4 DFT-computed energies (in Ha) of Fe(III) porphine species and ligands [a]

	E (vacuum)[b]			Zero Point Energy (vacuum)			E (*n*-octanol)[c]
Ligands							
H_2O	−76.41187			0.020765			−76.4767128
HO^-	−75.760216			0.007599			−75.9574764788
HOAc	−229.036116497			0.060802			−229.168163359
$^-$OAc	−228.441555639			0.047838			−228.699277251
Complexes							
	Spin State			**Spin State**			
	$^5/_2$	**$^3/_2$**	**$^1/_2$**	**$^5/_2$**	**$^3/_2$**	**$^1/_2$**	
FeP	−1111.259607	***−1111.268546***	−1111.239737	0.272745	0.277925	0.279093	−2252.26439868
H_2O-FeP	−1187.62860	***−1187.690788***	−1187.68208	0.297009	0.302064	0.300159	−2328.74015117
H_2O-FeP-HOAc	−1416.705221	***−1416.705503***	−1416.699155	0.362015	0.363772	0.366087	−2557.90958963
H_2O-FeP-OAc	−1416.294926	***−1416.322709***	−1416.319396	0.345888	0.351159	0.353647	−2557.46221497
HO-FeP	***−1187.312712***	−1187.303995	−1187.295842	0.287462	0.289307	0.29089	−2328.28507271
HO-FeP-HOAc	***−1416.30560***	−1416.299186	−1416.297417	0.348913	0.350844	0.353462	−2557.44487837
HO-FeP-OAc	−1415.79171	−1415.780802	***−1415.792308***	0.335794	0.337549	0.340618	−2556.98130355
FeP-HOAc	−1340.28694	***−1340.297270***	−1340.281844	0.338235	0.340690	0.337555	−2481.44092454
FeP-OAc	***−1339.918022***	−1339.846604	−1339.902792	0.326489	0.323932	0.328545	−2480.99666277

[a] Lowest energy spin states are italicised in bold; [b] B3LYP/LANL2DZ with zero point energy correction; [b] B3LYP/6-311++G(d,p) performed on the structure having the lowest energy spin state (ground state) in vacuum. Calculations were conducted using the SMD implicit solvent model.

Table S5 DFT-computed reaction energies (kcal mol^{-1}) of Fe(III) porphine (FeP) species in *n*-octanol. [a]

	Δ Energy	
	X = water	**X = hydroxide**
X-FeP + HOAc → X-FeP-HOAc	−0.23	5.65
X-FeP + HOAc → FeP + X + HOAc	3.29	38.44
X-FeP + HOAc → FeP-HOAc + X	−0.72	34.42
X-FeP + $^{-}$OAc → X-FeP-OAc	−13.51	5.25
X-FeP + $^{-}$OAc → FeP + X + $^{-}$OAc	3.29	38.44
X-FeP + $^{-}$OAc → FeP-OAc + X	−16.95	18.20

[a] Energies of individual species were calculated by adding B3LYP/LANL2DZ zero point energies of ground spin state species to B3LYP/LANL2DZ(d,p) single point energies reported in Table S4

Table S6 Coordinates of geometry optimised (B3LYP/LANL2DZ) FeP species with acetate/acetic acid molecules initially placed at 3.4 Å from the iron centre [a]

Atom	X	Y	Z
		H_2O-FeP-OAc	
O	0.27458	-0.01926	-2.44611
H	0.67385	0.79331	-2.81878
H	-0.55044	-0.24017	-2.92432
Fe	0.09902	-0.01427	-0.16348
N	1.54763	1.4763	-0.28416
N	-1.37225	1.43004	-0.47234
N	-1.3134	-1.49402	-0.4882
N	1.60017	-1.44785	-0.21372
C	2.92501	1.29097	-0.18664
C	3.57838	2.59061	-0.15852
C	2.58763	3.54972	-0.23087
C	1.31409	2.85054	-0.30692
C	-1.18563	2.80989	-0.47407
C	-2.48064	3.46408	-0.59296
C	-3.43599	2.47026	-0.66807
C	-2.73879	1.19488	-0.59575
C	-2.69018	-1.30894	-0.60498

C	-3.34019	-2.60871	-0.66063
C	-2.35031	-3.56706	-0.57117
C	-1.07969	-2.8678	-0.4598
C	1.41504	-2.82678	-0.23871
C	2.71305	-3.48226	-0.16223
C	3.6697	-2.48907	-0.1031
C	2.96951	-1.21288	-0.14048
C	3.58066	0.05073	-0.12219
C	0.05395	3.46486	-0.3932
C	-3.34634	-0.06936	-0.65496
C	0.17765	-3.48186	-0.34381
C	-0.27002	0.1771	4.17957
C	-0.85968	0.02879	2.78812
O	0.04797	0.02672	1.80689
O	-2.10528	-0.08643	2.59218
H	-4.50878	2.58208	-0.76118
H	-4.42906	-0.09024	-0.74544
H	-4.40847	-2.76042	-0.74873
H	-2.46285	-4.64379	-0.57394
H	0.19477	-4.56855	-0.34308
H	2.8637	-4.55435	-0.15981
H	4.74489	-2.60104	-0.04342
H	4.66521	0.07147	-0.05627
H	4.64819	2.74158	-0.08867
H	2.70089	4.62642	-0.23125
H	0.03737	4.55155	-0.40222
H	-2.63085	4.53604	-0.61424
H	-1.05823	0.18317	4.93735
H	0.30601	1.109	4.24047
H	0.42259	-0.65072	4.37756
	H_2O-FeP-HOAc		
O	0.166608	0.05675	0.13965
H	0.511587	-0.41863	0.920937
H	0.795597	0.729338	-0.18758
Fe	-1.6698	-0.32091	-0.75779
N	-2.64327	-1.67354	0.481124
N	-2.77802	1.195672	0.135773
N	-1.29031	0.974147	-2.32571
N	-1.2667	-1.90368	-2.05207
C	-2.55044	-3.06864	0.429814
C	-3.20263	-3.63957	1.591321
C	-3.70348	-2.59076	2.337389
C	-3.36503	-1.36652	1.639526
C	-3.48013	1.10292	1.342714
C	-3.90722	2.426462	1.757677

C	-3.46086	3.317875	0.804601
C	-2.7537	2.551216	-0.2043
C	-1.47654	2.361798	-2.33012
C	-0.90039	2.924559	-3.53588
C	-0.38308	1.877518	-4.27066
C	-0.63703	0.660252	-3.52457
C	-0.61796	-1.81718	-3.28685
C	-0.31617	-3.15122	-3.77115
C	-0.78005	-4.04367	-2.82711
C	-1.37011	-3.26668	-1.75315
C	-1.95315	-3.80415	-0.60084
C	-3.74076	-0.0795	2.043037
C	-2.14375	3.091999	-1.34169
C	-0.31513	-0.62881	-3.96125
C	-7.24816	-0.21873	-1.76211
C	-6.05734	0.361003	-2.48448
O	-4.88726	-0.05043	-2.39975
O	-6.30619	1.450436	-3.30575
H	-7.2503	1.725407	-3.3268
H	-3.59487	4.391457	0.777897
H	-2.21233	4.167262	-1.47969
H	-0.90684	3.977637	-3.78544
H	0.111262	1.915775	-5.23261
H	0.189329	-0.71665	-4.9193
H	0.179637	-3.36697	-4.70867
H	-0.73494	-5.1248	-2.84923
H	-1.961	-4.8863	-0.50678
H	-3.27317	-4.69976	1.79744
H	-4.2593	-2.63592	3.264936
H	-4.30335	0.005803	2.968377
H	-4.47339	2.635718	2.656091
H	-7.72166	0.548957	-1.13702
H	-6.93653	-1.05551	-1.13434
H	-7.99563	-0.56731	-2.4861

[a] Optimised in implicit *n*-octanol (SMD).

7. References.

1 J. M. Pisciotta, I. Coppens, A. K. Tripathi, P. F. Scholl, J. Schuman, S. Bajad, V. Shulaev and D. J. Sullivan, *Biochem. J.*, 2007, **402**, 197–204.

2 S. Pagola, P. W. Stephens, D. S. Bohle, A. D. Kosar and S. K. Madsen, *Nature*, 2000, **404**, 307–310.

3 D. Kuter, V. Streltsov, N. Davydova, G. A. Venter, K. J. Naidoo and T. J. Egan, *Inorg. Chem.*, 2014, **53**, 10811–10824.

4 J. Gildenhuys, T. le Roux, T. J. Egan and K. A. de Villiers, *J. Am. Chem. Soc.*, 2013, **135**, 1037–1047.

5 D. S. Bohle and E. L. Dodd, *Inorg. Chem.*, 2012, **51**, 4411–4413.

6 R. W. Pastor and A. D. MacKerell, *J. Phys. Chem. Lett.*, 2011, **2**, 1526–1532.